

Semileptonic B_c meson decays to S-wave charmonia and $X(3872)$ within the covariant light-front approach

Zhi-Jie Sun¹, Si-Yang Wang², Zhi-Qing Zhang¹ *, You-Ya Yang¹ and Zi-Yu Zhang¹

¹ *Institute of Theoretical Physics, School of Sciences,
Henan University of Technology, Zhengzhou, Henan 450052, China;*

² *Institute of Particle Physics and Key Laboratory of Quark and Lepton Physics (MOE),
Central China Normal University, Wuhan, Hubei 430079, China*

(Dated: August 8, 2023)

Abstract

In this work, we investigate the semileptonic decays of B_c meson to $\eta_c(1S, 2S, 3S)$, $\psi(1S, 2S, 3S)$ and $X(3872)$ within the framework of covariant light-front quark model (CLFQM). We combine the helicity amplitudes via the corresponding form factors to obtain the branching ratios of the semileptonic decays $B_c \rightarrow \eta_c(1S, 2S, 3S)\ell\nu_\ell$, $B_c \rightarrow \psi(1S, 2S, 3S)\ell\nu_\ell$ and $B_c \rightarrow X(3872)\ell\nu_\ell$ with $\ell = e, \mu, \tau$. In view of the $R_{J/\psi}$ anomaly released by the LHCb collaboration, it is necessary to calculate the ratios R_X with $X = \psi(1S, 2S, 3S), \eta_c(1S, 2S, 3S), X(3872)$ systematically, which are helpful to check the lepton flavor universality (LFU). Furthermore, we also take into account another two physical observables, one is the longitudinal polarization fraction f_L and the other is the forward-backward asymmetry A_{FB} , which can provide new clues to understand the $R_{J/\psi}$ anomaly. Such theoretical predictions are necessary and interesting, which can be tested in the future LHCb experiments.

PACS numbers: 13.25.Hw, 12.38.Bx, 14.40.Nd

* zhangzhiqing@haut.edu.cn (corresponding author)

I. INTRODUCTION

In this paper we research the exclusive semileptonic B_c decays to $\eta_c(1S, 2S, 3S)$, $\psi(1S, 2S, 3S)$ and $X(3872)$ by using the the covariant Light-Front quark model (CLFQM). The traditional light-front quark model (LFQM) was initially proposed by Terentev and Berestesky [1, 2], which is based on the light-front formalism of Hamiltonian dynamics [3], and later developed and applied to determinate the transition form factor, decay constant and distribution amplitude [4–6]. Unfortunately, the Lorentz covariance of the matrix element is lost and the zero-mode contributions can not be handled in the traditional LFQM. To compensate for these deficiencies, Jaus put forward the CLFQM [7], where the spurious contribution being dependent on the orientation of the light-front can be eliminated by the inclusion of the zero-mode contributions. This model has been used successfully to investigate the nonleptonic and simileptonic $B_{(c)}$ meson decays [8–12].

The semileptonic B_c meson decays to charmonium states play an important role in testing the Standard Model (SM) and searching for new physics (NP), for example, the issues about test of the lepton flavor universality (LFU), determination of the CKM matrix element V_{cb} are often searched by experiments and theories. In 2017, the ratio of the semileptonic branching fractions $R_{J/\psi}|_{\text{exp}}$ was measured by the LHCb Collaboration [13] ,

$$R_{J/\psi}|_{\text{exp}} = \frac{\mathcal{B}r(B_c^+ \rightarrow J/\psi\tau^+\nu_\tau)}{\mathcal{B}r(B_c^+ \rightarrow J/\psi\mu^+\nu_\mu)} = 0.71 \pm 0.17 \pm 0.18, \quad (1)$$

which lies within 2σ above the range of existing SM predictions [14, 15]. It was considered as one of the most fascinating puzzles in flavor physics in recent years. In order to provide a generalized and complementary check, it is useful to measure the values of $R_{\psi(2S,3S)}$ and $R_{\eta_c(1S,2S,3S)}$. At present, there also exist some results about these ratios predicted by other approaches. Furthermore, another two physical measurements are also sensitive to NP, one is the longitudinal polarization fraction f_L and the other is the forward-backward asymmetry A_{FB} . These observations can be represented by the helicity amplitudes, which are combined via the corresponding form factors.

Many different theoretical methods have been devoted to studying the semileptonic B_c meson decays to charmonium states, such as the nonrelativistic QCD (NRQCD) [16, 17], the Bethe-Salpeter (BS) method [18, 19], the relativistic quark model (RQM)[20–22], the light-cone QCD sum rules[23, 24], the relativistic constituent quark model (RCQM) [25, 26], the non-relativistic quark model (NRQM)[27], the QCD potential model(QCDPM)[28], the Isgur-Scora-Grinstein-Wise (ISGW2) quark model[29], the perturbative QCD (PQCD) approach [30–32], the covariant confined quark model (CCQM) [33], the QCD sum rules (QCDSR) [34], the covariant quark model (CQM)[35], the relativistic independent quark (RIQ) model[36], and so on.

This paper is organized as follows. In section II, the formalism of the CLFQM and the helicity amplitudes combined via form factors are presented. Numerical results for the branching ratios, the longitudinal polarization fractions f_L and the forward-backward asymmetries A_{FB} for these semileptonic B_c decays are listed in section III. Detailed comparisons with other theoretical values and relevant discussions are also included. The summary is presented in section IV. Some specific rules when performing the p^- integration and analytical expressions of the $B_c \rightarrow \eta_c(1S, 2S, 3S), \psi(1S, 2S, 3S), X(3872)$ transition form factors are collected in Appendix A and B, respectively.

II. FORMALISM

A. Covariant Light-Front Quark Model

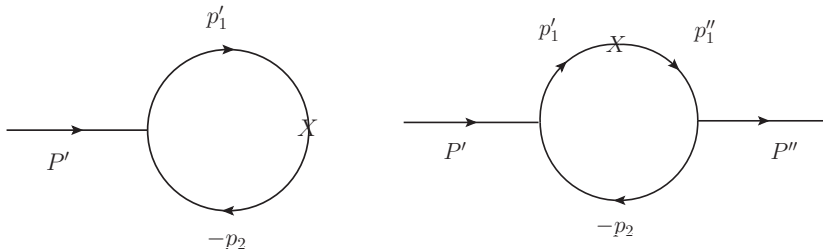


FIG. 1: Feynman diagrams for B_c decay (left) and transition (right) amplitudes, where $P^{(m)}$ is the incoming (outgoing) meson momentum, $p_1^{(m)}$ is the quark momentum, p_2 is the anti-quark momentum. The X in the diagrams denotes the vector or axial-vector transition vertex.

In the covariant light-front quark model, we will employ the light-front decomposition of the momentum $p = (p^-, p^+, p_\perp)$ with $p^\pm = p^0 \pm p_z, p^2 = p^+ p^- - p_\perp^2$. The Feynman diagrams for B_c meson decay and transition amplitudes are shown in Fig. 1. The incoming (outgoing) meson has the mass $M'(M'')$ with the momentum $P' = p'_1 + p_2 (P'' = p''_1 + p_2)$, where $p_1^{(m)}$ and p_2 are the momenta of the quark and anti-quark inside the incoming (outgoing) meson with the mass $m_1^{(m)}$ and m_2 , respectively. Here we use the same notations as those in Refs. [7, 11] and M' refers to m_{B_c} for B_c meson decays. These momenta can be expressed in terms of the internal variables (x_i, p'_\perp) as

$$p_{1,2}^+ = x_{1,2} P'^+, \quad p'_{1,2\perp} = x_{1,2} P'_\perp \pm p'_\perp, \quad (2)$$

TABLE I: Feynman rules for the vertices $i\Gamma'_M$ of the incoming meson-quark-antiquark, where p'_1 and p_2 are the quark and antiquark momenta, respectively. It is noticed that for the outgoing meson, we should use $i(\gamma_0\Gamma_M^\dagger\gamma_0)$ for the relevant vertices.

| M ($^{2S+1}L_J$) | $i\Gamma'_M$ |
|----------------------|--|
| η_c (1S_0) | $H'_{\eta_c}\gamma_5$ |
| ψ (3S_1) | $iH'_\psi\left[\gamma_\mu - \frac{1}{W'_\psi}(p'_1 - p_2)_\mu\right]$ |
| X (3P_1) | $-iH'_X\left[\gamma_\mu + \frac{1}{W'_X}(p'_1 - p_2)_\mu\right]\gamma_5$ |

where $x_1 + x_2 = 1$. Using these internal variables, we can define some quantities for the incoming meson which will be used in the following calculations

$$\begin{aligned}
M_0'^2 &= (e'_1 + e_2)^2 = \frac{p_\perp'^2 + m_1'^2}{x_1} + \frac{p_\perp'^2 + m_2'^2}{x_2}, & \widetilde{M}'_0 &= \sqrt{M_0'^2 - (m_1' - m_2')^2}, \\
e_i^{(\prime)} &= \sqrt{m_i^{(\prime)2} + p_\perp'^2 + p_z'^2}, & p_z' &= \frac{x_2 M_0'}{2} - \frac{m_2'^2 + p_\perp'^2}{2x_2 M_0'},
\end{aligned} \tag{3}$$

where M_0' is the kinetic invariant mass of the incoming meson and can be expressed as the energies of the quark and the anti-quark $e_i^{(\prime)}$. It is similar to the case of the outgoing meson. To calculate the amplitudes for the transition form factors, we need the Feynman rules for the meson-quark-antiquark vertices ($i\Gamma'_M$ ($M = \eta_c, \psi, X$)), which are listed in Tab. I. Here $X(3872)$ is considered as a 1^{++} charmonium state in our calculations [37] and replaced with X in some places for simply.

B. Wave Functions and Decay Constants

In order to calculate the form factors, we need to specify the light-front wave functions. In principle, one can obtain them by solving the relativistic Schrödinger equation. But it is difficult to obtain the exact solution in many cases. Usually, the Gaussian-type and harmonic-oscillator-type wave functions are used to describe various hadronic structures in many works. In the present work, we shall use the phenomenological Gaussian-type wave functions

$$\begin{aligned}
\varphi' &= \varphi'(x_2, p'_\perp) = 4 \left(\frac{\pi}{\beta'^2}\right)^{\frac{3}{4}} \sqrt{\frac{dp'_z}{dx_2}} \exp\left(-\frac{p_z'^2 + p_\perp'^2}{2\beta'^2}\right), \\
\varphi'_p &= \varphi'_p(x_2, p'_\perp) = \sqrt{\frac{2}{\beta'^2}}\varphi', & \frac{dp'_z}{dx_2} &= \frac{e'_1 e_2}{x_1 x_2 M_0'},
\end{aligned} \tag{4}$$

where the parameter β' describes the momentum distribution and is about of order Λ_{QCD} . It is usually determined by the decay constants through the analytic expressions in the conventional light-front approach, which are given as follows [7, 11]

$$f_{\eta_c} = \frac{N_c}{16\pi^3} \int dx_2 d^2 p'_\perp \frac{h'_{\eta_c}}{x_1 x_2 (M'^2 - M_0'^2)} 4(m'_1 x_2 + m_2 x_1), \quad (5)$$

$$f_\psi = \frac{N_c}{4\pi^3 M'} \int dx_2 d^2 p'_\perp \frac{h'_\psi}{x_1 x_2 (M'^2 - M_0'^2)} \times \left[x_1 M_0'^2 - m'_1 (m'_1 - m_2) - p'^2_\perp + \frac{m'_1 + m_2}{w'_\psi} p'^2_\perp \right], \quad (6)$$

$$f_X = -\frac{N_c}{4\pi^3 M'} \int dx_2 d^2 p'_\perp \frac{h'_X}{x_1 x_2 (M'^2 - M_0'^2)} \times \left[x_1 M_0'^2 - m'_1 (m'_1 + m_2) - p'^2_\perp - \frac{m'_1 - m_2}{w'_X} p'^2_\perp \right], \quad (7)$$

where m'_1 and m_2 are the constituent quarks of meson M ($M = \eta_c, \psi, X$), and M'_0 is defined in Eq. (3). The explicit forms of h'_M are given by [11]

$$h'_{\eta_c} = h'_\psi = (M'^2 - M_0'^2) \sqrt{\frac{x_1 x_2}{N_c}} \frac{1}{\sqrt{2\widetilde{M}'_0}} \varphi', \quad (8)$$

$$\sqrt{\frac{2}{3}} h'_X = (M'^2 - M_0'^2) \sqrt{\frac{x_1 x_2}{N_c}} \frac{1}{\sqrt{2\widetilde{M}'_0}} \frac{\widetilde{M}'_0}{2\sqrt{3}\widetilde{M}'_0} \varphi'_p, \quad (9)$$

where φ' and φ'_p are the light-front momentum distribution amplitudes for the S-wave and P-wave mesons, respectively, defined in Eq. (4).

C. Helicity amplitudes and Observables

Since the form factors involving the fitted parameters for the $B_c \rightarrow \eta_c(1S, 2S, 3S)$, $B_c \rightarrow \psi(1S, 2S, 3S)$ and $B_c \rightarrow X(3872)$ transitions have been investigated in our recent work [8], so it is convenient to obtain the differential decay widths of these semileptonic B_c decays by the combination of the helicity amplitudes via form factors, which are listed as following

$$\frac{d\Gamma(B_c \rightarrow \eta_c \ell \nu_\ell)}{dq^2} = \left(\frac{q^2 - m_\ell^2}{q^2}\right)^2 \frac{\sqrt{\lambda(m_{B_c}^2, m_{\eta_c}^2, q^2)} G_F^2 |V_{cb}|^2}{384 m_{B_c}^3 \pi^3} \times \frac{1}{q^2} \times \left\{ (m_\ell^2 + 2q^2) \lambda(m_{B_c}^2, m_{\eta_c}^2, q^2) F_1^2(q^2) + 3m_\ell^2 (m_{B_c}^2 - m_{\eta_c}^2)^2 F_0^2(q^2) \right\}, \quad (10)$$

$$\frac{d\Gamma_L(B_c \rightarrow \psi \ell \nu_\ell)}{dq^2} = \left(\frac{q^2 - m_\ell^2}{q^2}\right)^2 \frac{\sqrt{\lambda(m_{B_c}^2, m_\psi^2, q^2)} G_F^2 |V_{cb}|^2}{384 m_{B_c}^3 \pi^3} \times \frac{1}{q^2} \left\{ 3m_\ell^2 \lambda(m_{B_c}^2, m_\psi^2, q^2) A_0^2(q^2) + (m_\ell^2 + 2q^2) \times \left| \frac{1}{2m_\psi} \left[(m_{B_c}^2 - m_\psi^2 - q^2)(m_{B_c} + m_\psi) A_1(q^2) - \frac{\lambda(m_{B_c}^2, m_\psi^2, q^2)}{m_{B_c} + m_\psi} A_2(q^2) \right] \right|^2 \right\}, \quad (11)$$

$$\begin{aligned} \frac{d\Gamma_{\pm}(B_c \rightarrow \psi \ell \nu_{\ell})}{dq^2} &= \left(\frac{q^2 - m_{\ell}^2}{q^2}\right)^2 \frac{\sqrt{\lambda(m_{B_c}^2, m_{\psi}^2, q^2)} G_F^2 |V_{cb}|^2}{384 m_{B_c}^3 \pi^3} \\ &\times \left\{ (m_{\ell}^2 + 2q^2) \lambda(m_{B_c}^2, m_{\psi}^2, q^2) \left| \frac{V(q^2)}{m_{B_c} + m_{\psi}} \mp \frac{(m_{B_c} + m_{\psi}) A_1(q^2)}{\sqrt{\lambda(m_{B_c}^2, m_{\psi}^2, q^2)}} \right|^2 \right\}, \end{aligned} \quad (12)$$

$$\begin{aligned} \frac{d\Gamma_L(B_c \rightarrow X \ell \nu_{\ell})}{dq^2} &= \left(\frac{q^2 - m_{\ell}^2}{q^2}\right)^2 \frac{\sqrt{\lambda(m_{B_c}^2, m_X^2, q^2)} G_F^2 |V_{cb}|^2}{384 m_{B_c}^3 \pi^3} \times \frac{1}{q^2} \{ 3m_{\ell}^2 \lambda(m_{B_c}^2, m_X^2, q^2) V_0^2(q^2) + (m_{\ell}^2 + 2q^2) \\ &\times \left| \frac{1}{2m_X} \left[(m_{B_c}^2 - m_X^2 - q^2)(m_{B_c} - m_X) V_1(q^2) - \frac{\lambda(m_{B_c}^2, m_X^2, q^2)}{m_{B_c} - m_X} V_2(q^2) \right] \right|^2 \}, \end{aligned} \quad (13)$$

$$\begin{aligned} \frac{d\Gamma_{\pm}(B_c \rightarrow X \ell \nu_{\ell})}{dq^2} &= \left(\frac{q^2 - m_{\ell}^2}{q^2}\right)^2 \frac{\sqrt{\lambda(m_{B_c}^2, m_X^2, q^2)} G_F^2 |V_{cb}|^2}{384 m_{B_c}^3 \pi^3} \\ &\times \left\{ (m_{\ell}^2 + 2q^2) \lambda(m_{B_c}^2, m_X^2, q^2) \left| \frac{A(q^2)}{m_{B_c} - m_X} \mp \frac{(m_{B_c} - m_X) V_1(q^2)}{\sqrt{\lambda(m_{B_c}^2, m_X^2, q^2)}} \right|^2 \right\}, \end{aligned} \quad (14)$$

where $\lambda(q^2) = \lambda(m_{B_c}^2, m_{\eta_c(\psi, X)}^2, q^2) = (m_{B_c}^2 + m_{\eta_c(\psi, X)}^2 - q^2)^2 - 4m_{B_c}^2 m_{\eta_c(\psi, X)}^2$ and m_{ℓ} is the mass of the lepton ℓ with $\ell = e, \mu, \tau$ ¹. It is noticed that although the electron and muon are very light compared with the charm quark, we do not ignore their masses in our calculations.

The combined transverse and total differential decay widths are defined as

$$\frac{d\Gamma_T}{dq^2} = \frac{d\Gamma_+}{dq^2} + \frac{d\Gamma_-}{dq^2}, \quad \frac{d\Gamma}{dq^2} = \frac{d\Gamma_L}{dq^2} + \frac{d\Gamma_T}{dq^2}. \quad (15)$$

For $\psi(1S, 2S, 3S)$ and $X(3872)$, it is meaningful to define the polarization fraction due to the existence of different polarizations

$$f_L = \frac{\Gamma_L}{\Gamma_L + \Gamma_+ + \Gamma_-}. \quad (16)$$

As to the forward-backward asymmetry, the analytical expression is defined as [38],

$$A_{FB} = \frac{\int_0^1 \frac{d\Gamma}{d\cos\theta} d\cos\theta - \int_{-1}^0 \frac{d\Gamma}{d\cos\theta} d\cos\theta}{\int_{-1}^1 \frac{d\Gamma}{d\cos\theta} d\cos\theta} = \frac{\int b_{\theta}(q^2) dq^2}{\Gamma_{B_c}}, \quad (17)$$

where θ is the angle between the 3-momenta of the lepton ℓ and the initial B_c meson in the $\ell\nu$ rest frame. The function $b_{\theta}(q^2)$ represents the angular coefficient, which can be written as [38]

$$b_{\theta}^{(\eta_c)}(q^2) = \frac{G_F^2 |V_{cb}|^2}{128 \pi^3 m_{B_c}^3} q^2 \sqrt{\lambda(q^2)} \left(1 - \frac{m_{\ell}^2}{q^2}\right)^2 \frac{m_{\ell}^2}{q^2} (H_{V,0}^s H_{V,t}^s), \quad (18)$$

$$b_{\theta}^{(\psi, X)}(q^2) = \frac{G_F^2 |V_{cb}|^2}{128 \pi^3 m_{B_c}^3} q^2 \sqrt{\lambda(q^2)} \left(1 - \frac{m_{\ell}^2}{q^2}\right)^2 \left[\frac{1}{2} (H_{V,+}^2 - H_{V,-}^2) + \frac{m_{\ell}^2}{q^2} (H_{V,0} H_{V,t}) \right], \quad (19)$$

¹ For now on, we use ℓ to represent e, μ, τ and use ℓ' to represent e, μ for simplicity.

where the helicity amplitudes

$$H_{V,0}^s(q^2) = \sqrt{\frac{\lambda(q^2)}{q^2}} F_1(q^2), H_{V,t}^s(q^2) = \frac{m_{B_c}^2 - m_{\eta_c}^2}{\sqrt{q^2}} F_0(q^2), \quad (20)$$

for the B_c to $\eta_c(1S, 2S, 3S)$ meson transitions, and the helicity amplitudes

$$\begin{aligned} H_{V,\pm}(q^2) &= (m_{B_c} + m_\psi) A_1(q^2) \mp \frac{\sqrt{\lambda(q^2)}}{m_{B_c} + m_\psi} V(q^2), \\ H_{V,0}(q^2) &= \frac{m_{B_c} + m_\psi}{2m_\psi \sqrt{q^2}} \left[- (m_{B_c}^2 - m_\psi^2 - q^2) A_1(q^2) + \frac{\lambda(q^2) A_2(q^2)}{(m_{B_c} + m_\psi)^2} \right], \\ H_{V,t}(q^2) &= -\sqrt{\frac{\lambda(q^2)}{q^2}} A_0(q^2), \end{aligned} \quad (21)$$

for the B_c to $\psi(1S, 2S, 3S)$ transitions, and the helicity amplitudes

$$\begin{aligned} H_{V,\pm}(q^2) &= (m_{B_c} - m_X) V_1(q^2) \mp \frac{\sqrt{\lambda(q^2)}}{m_{B_c} - m_X} A(q^2), \\ H_{V,0}(q^2) &= \frac{m_{B_c} - m_X}{2m_X \sqrt{q^2}} \left[- (m_{B_c}^2 - m_X^2 - q^2) V_1(q^2) + \frac{\lambda(q^2) V_2(q^2)}{(m_{B_c} - m_X)^2} \right], \\ H_{V,t}(q^2) &= -\sqrt{\frac{\lambda(q^2)}{q^2}} V_0(q^2), \end{aligned} \quad (22)$$

for the B_c to $X(3872)$ transition. It is noticed that the subscript V in each helicity amplitude refers to the $\gamma_\mu(1 - \gamma_5)$ current. The transition form factors are collected in Appendix B.

III. NUMERICAL RESULTS AND DISCUSSIONS

The adopted input parameters [39], such as the constituent quark masses, the hadron and lepton masses, the B_c meson life and the Cabibbo-Kobayashi-Maskawa (CKM) matrix element V_{cb} , in our numerical calculations are listed in Table II. In the calculations of the helicity amplitudes, the transition form factors are the most important inputs, which have been calculated in our previous work [8]. Those parameterized form factors are extrapolated from the space-like region to the time-like region by using following expression,

TABLE II: The values of the input parameters.

| | | | | | |
|------------------|--|---------------------------|--------------------------|--|-----------------|
| Mass(GeV) | $m_b = 4.8$ | $m_c = 1.4$ | $m_e = 0.000511$ | $m_\mu = 0.106$ | $m_\tau = 1.78$ |
| | $m_{J/\psi} = 3.0969$ | $m_{\psi(2S)} = 3.6861$ | $m_{\psi(3S)} = 4.039$ | $M_{B_c} = 6.27447$ | |
| | $m_{\eta_c} = 2.9839$ | $m_{\eta_c(2S)} = 3.6375$ | $m_{\eta_c(3S)} = 3.940$ | $m_{X(3872)} = 3.87165$ | |
| CKM | $V_{cb} = (40.8 \pm 1.4) \times 10^{-3}$ | | Lifetime | $\tau_{B_c} = (0.510 \pm 0.009) \times 10^{-12}\text{s}$ | |

$$F(q^2) = F(0)\exp\left(a\frac{q^2}{m_{B_c}^2} + b\left(\frac{q^2}{m_{B_c}^2}\right)^2\right) \quad (23)$$

where $F(q^2)$ denotes different form factors. The corresponding results are listed in Tab. III.

TABLE III: $B_c \rightarrow \eta_c(1S, 2S, 3S), \psi(1S, 2S, 3S), X(3872)$ form factors in the CLFQM. The uncertainties are from the decay constants of B_c and the final state mesons.

| $B_c \rightarrow \eta_c$ | | | $B_c \rightarrow J/\psi$ | | | |
|------------------------------|----------------------------------|-----------------------------------|-----------------------------------|-----------------------------------|-----------------------------------|-----------------------------------|
| | F_1 | F_0 | V | A_0 | A_1 | A_2 |
| $F(0)$ | $0.60^{+0.00+0.01}_{-0.00-0.01}$ | $0.60^{+0.00+0.01}_{-0.01-0.00}$ | $0.76^{+0.00+0.04}_{-0.00-0.04}$ | $0.55^{+0.00+0.03}_{-0.00-0.04}$ | $0.53^{+0.00+0.02}_{-0.03-0.00}$ | $0.49^{+0.00+0.00}_{-0.00-0.01}$ |
| $F(q_{max}^2)$ | $1.06^{+0.00+0.03}_{-0.00-0.03}$ | $0.85^{+0.00+0.02}_{-0.01-0.02}$ | $1.37^{+0.00+0.11}_{-0.00-0.10}$ | $0.76^{+0.00+0.06}_{-0.00-0.07}$ | $0.78^{+0.01+0.02}_{-0.01-0.05}$ | $0.84^{+0.00+0.03}_{-0.00-0.00}$ |
| a | $1.95^{+0.01+0.03}_{-0.01-0.03}$ | $1.44^{+0.00+0.03}_{-0.00-0.03}$ | $2.16^{+0.01+0.09}_{-0.01-0.08}$ | $1.22^{+0.02+0.07}_{-0.02-0.07}$ | $1.45^{+0.03+0.09}_{-0.01-0.09}$ | $1.97^{+0.01+0.11}_{-0.01-0.11}$ |
| b | $0.48^{+0.00+0.01}_{-0.00-0.01}$ | $-0.62^{+0.02+0.02}_{-0.02-0.03}$ | $0.53^{+0.00+0.01}_{-0.00-0.01}$ | $0.16^{+0.00+0.00}_{-0.00-0.00}$ | $0.29^{+0.00+0.02}_{-0.00-0.00}$ | $0.43^{+0.00+0.03}_{-0.00-0.03}$ |
| $B_c \rightarrow \eta_c(2S)$ | | | $B_c \rightarrow \psi(2S)$ | | | |
| | F_1 | F_0 | V | A_0 | A_1 | A_2 |
| $F(0)$ | $0.37^{+0.00+0.12}_{-0.00-0.18}$ | $0.37^{+0.00+0.12}_{-0.00-0.18}$ | $0.57^{+0.00+0.01}_{-0.00-0.00}$ | $0.41^{+0.00+0.00}_{-0.00-0.00}$ | $0.35^{+0.00+0.00}_{-0.00-0.00}$ | $0.17^{+0.00+0.00}_{-0.00-0.00}$ |
| $F(q_{max}^2)$ | $0.48^{+0.00+0.28}_{-0.00-0.31}$ | $0.41^{+0.00+0.28}_{-0.01-0.28}$ | $0.67^{+0.00+0.02}_{-0.00-0.00}$ | $0.44^{+0.00+0.00}_{-0.00-0.00}$ | $0.35^{+0.00+0.00}_{-0.00-0.00}$ | $0.12^{+0.00+0.00}_{-0.00-0.00}$ |
| a | $1.44^{+0.00+0.92}_{-0.00-0.66}$ | $0.73^{+0.01+0.99}_{-0.01-0.95}$ | $1.01^{+0.01+0.01}_{-0.01-0.02}$ | $0.39^{+0.01+0.01}_{-0.01-0.01}$ | $0.08^{+0.01+0.02}_{-0.02-0.03}$ | $-1.53^{+0.07+0.09}_{-0.09-0.13}$ |
| b | $0.15^{+0.02+0.50}_{-0.02-0.34}$ | $-0.81^{+0.02+0.34}_{-0.02-0.28}$ | $-0.16^{+0.03+0.01}_{-0.03-0.02}$ | $-0.15^{+0.02+0.01}_{-0.02-0.01}$ | $-0.69^{+0.03+0.01}_{-0.04-0.02}$ | $-3.67^{+0.14+0.13}_{-0.19-0.21}$ |
| $B_c \rightarrow \eta_c(3S)$ | | | $B_c \rightarrow \psi(3S)$ | | | |
| | F_1 | F_0 | V | A_0 | A_1 | A_2 |
| $F(0)$ | $0.29^{+0.00+0.04}_{-0.00-0.05}$ | $0.29^{+0.00+0.04}_{-0.00-0.05}$ | $0.46^{+0.00+0.02}_{-0.00-0.02}$ | $0.31^{+0.00+0.01}_{-0.00-0.01}$ | $0.27^{+0.00+0.01}_{-0.00-0.01}$ | $0.14^{+0.00+0.01}_{-0.00-0.01}$ |
| $F(q_{max}^2)$ | $0.36^{+0.00+0.07}_{-0.00-0.08}$ | $0.32^{+0.00+0.07}_{-0.00-0.08}$ | $0.53^{+0.00+0.03}_{-0.00-0.03}$ | $0.33^{+0.00+0.01}_{-0.00-0.01}$ | $0.28^{+0.00+0.02}_{-0.00-0.01}$ | $0.12^{+0.00+0.02}_{-0.00-0.02}$ |
| a | $1.53^{+0.00+0.29}_{-0.00-0.23}$ | $0.85^{+0.01+0.44}_{-0.01-0.31}$ | $1.14^{+0.03+0.04}_{-0.03-0.03}$ | $0.49^{+0.03+0.03}_{-0.02-0.03}$ | $0.25^{+0.02+0.04}_{-0.02-0.03}$ | $-1.01^{+0.02+0.04}_{-0.02-0.04}$ |
| b | $0.23^{+0.01+0.13}_{-0.01-0.13}$ | $-0.74^{+0.01+0.05}_{-0.00-0.24}$ | $-0.01^{+0.01+0.01}_{-0.01-0.01}$ | $-0.04^{+0.01+0.01}_{-0.01-0.01}$ | $-0.45^{+0.01+0.00}_{-0.01-0.00}$ | $-2.73^{+0.01+0.00}_{-0.01-0.00}$ |
| $B_c \rightarrow X(3872)$ | | | A | V_0 | V_1 | V_2 |
| $F(0)$ | | | $0.28^{+0.00+0.02}_{-0.00-0.03}$ | $0.21^{+0.00+0.01}_{-0.00-0.01}$ | $1.13^{+0.00+0.01}_{-0.00-0.01}$ | $0.11^{+0.00+0.01}_{-0.01-0.01}$ |
| $F(q_{max}^2)$ | | | $0.37^{+0.00+0.03}_{-0.00-0.04}$ | $0.19^{+0.00+0.02}_{-0.00-0.02}$ | $1.10^{+0.00+0.05}_{-0.00-0.06}$ | $0.12^{+0.00+0.01}_{-0.01-0.01}$ |
| a | | | $1.85^{+0.02+0.09}_{-0.02-0.08}$ | $-0.52^{+0.01+0.38}_{-0.01-0.32}$ | $-0.05^{+0.01+0.24}_{-0.01-0.20}$ | $0.77^{+0.03+0.04}_{-0.03-0.04}$ |
| b | | | $0.38^{+0.01+0.01}_{-0.01-0.03}$ | $-1.45^{+0.02+0.36}_{-0.03-0.32}$ | $-1.03^{+0.00+0.15}_{-0.00-0.12}$ | $-0.61^{+0.02+0.08}_{-0.02-0.12}$ |

The branching ratios for these semileptonic B_c decays to the S-wave ground charmonium states are collected in Tab. IV. The uncertainties arise from the B_c meson lifetime, the decay constants of B_c and final state mesons, respectively. Obviously, because the mass of τ lepton is much larger than those of e, μ leptons, $\mathcal{B}r(B_c^+ \rightarrow \eta_c(J/\Psi)\ell'^+\nu_{\ell'})$ are about $3 \sim 4$ times larger than $\mathcal{B}r(B_c^+ \rightarrow \eta_c(J/\Psi)\tau^+\nu_{\tau})$. For comparison, we also list the results calculated by other approaches. The predictions given by the NRQCD [16, 17] and the PQCD approach [30] are much larger than others. It is because that the former involves the large QCD correction K factor and the NLO charmonium wave functions, and the latter includes the

large weak transition form factors. These differences can be clarified by the future LHCb experiments. Certainly, our predictions are consistent with most of other theoretical results, such as the BS equation [18], the RQM [20–22], the RCQM [25, 26], the NRQM [27], the QCDDM [28], the CQM [35] and so on.

TABLE IV: Branching ratios (in%) of the semileptonic B_c decays to η_c and J/Ψ .

| | $\mathcal{B}r(B_c^+ \rightarrow \eta_c e^+ \nu_e)$ | $\mathcal{B}r(B_c^+ \rightarrow \eta_c \mu^+ \nu_\mu)$ | $\mathcal{B}r(B_c^+ \rightarrow \eta_c \tau^+ \nu_\tau)$ | $\mathcal{B}r(B_c^+ \rightarrow J/\psi e^+ \nu_e)$ | $\mathcal{B}r(B_c^+ \rightarrow J/\psi \mu^+ \nu_\mu)$ | $\mathcal{B}r(B_c^+ \rightarrow J/\psi \tau^+ \nu_\tau)$ |
|-----------|--|--|--|--|--|--|
| This work | $0.71^{+0.01+0.00+0.03}_{-0.01-0.00-0.03}$ | $0.69^{+0.01+0.00+0.03}_{-0.01-0.00-0.03}$ | $0.20^{+0.00+0.00+0.01}_{-0.00-0.01-0.01}$ | $1.60^{+0.03+0.01+0.19}_{-0.03-0.19-0.04}$ | $1.59^{+0.03+0.01+0.19}_{-0.03-0.20-0.04}$ | $0.40^{+0.01+0.00+0.05}_{-0.01-0.04-0.02}$ |
| [16, 17] | 2.1 | 2.1 | 0.64 | 6.7 | 6.7 | 0.52 |
| [18] | 0.55 | – | – | 1.73 | – | – |
| [20, 21] | 0.42 | – | – | 1.23 | – | – |
| [22] | 0.81 | – | 0.22 | 2.07 | – | 0.49 |
| [24] | 1.64 | – | 0.49 | 2.37 | – | 0.65 |
| [9] | 0.67 | 0.67 | 0.19 | 1.49 | 1.49 | 0.37 |
| [27] | 0.48 | 0.48 | 0.17 | 1.54 | 1.54 | 0.41 |
| [28] | 0.15 | – | – | 1.5 | – | – |
| [35] | 0.95 | 0.95 | 0.24 | 1.67 | 1.67 | 0.40 |
| [30] | 4.5 | 4.5 | 2.8 | 5.7 | 5.7 | 1.7 |
| [33] | 0.98 | – | 0.27 | 2.30 | – | 0.59 |
| [34, 49] | 0.75 | 0.75 | 0.23 | 1.9 | 1.9 | 0.48 |
| [50] | 0.97 | – | – | 2.35 | – | – |
| [25, 26] | 0.59 | 0.59 | 0.20 | 1.20 | 1.20 | 0.34 |
| [31] | 0.44 | 0.44 | 0.14 | 1.01 | 1.01 | 0.29 |
| [51] | 0.42 | 0.42 | 0.16 | 1.31 | 1.30 | 0.37 |

From Tab. IV, one can find that the value of the ratio $R_{J/\psi}$

$$R_{J/\psi} = \frac{\mathcal{B}r(B_c^+ \rightarrow J/\psi \tau^+ \nu_\tau)}{\mathcal{B}r(B_c^+ \rightarrow J/\psi \mu^+ \nu_\mu)} = 0.25 \pm 0.04, \quad (24)$$

which is fall in the range of $0.24 \leq R_{J/\psi} \leq 0.28$ predicted by most of other SM approaches, and is also consistent with the model-independent constraint $0.20 \leq R_{J/\psi} \leq 0.39$ [14]. Our prediction is smaller than the measured one shown in Eq. (1), but still agrees with it within 2σ errors. As a complementary check, we also calculate the value of R_{η_c} ,

$$R_{\eta_c} = \frac{\mathcal{B}r(B_c^+ \rightarrow \eta_c \tau^+ \nu_\tau)}{\mathcal{B}r(B_c^+ \rightarrow \eta_c \mu^+ \nu_\mu)} = 0.29 \pm 0.02, \quad (25)$$

which is still consistent with most of other theoretical results lying in range of $0.25 \leq R_{\eta_c} \leq 0.35$ [40], and agrees well with the model-independent prediction 0.29 ± 0.05 [41].

TABLE V: Branching ratios of the semileptonic B_c decays to the radially excited charmonium states.

| Reference | This work | [18] | [20, 21] | [23] | [28] | [29] | [30] |
|---|---|------|----------|------|------|------|-------|
| $10^{-3} \times \mathcal{B}r(B_c^+ \rightarrow \eta_c(2S)e^+\nu_e)$ | $0.91^{+0.02+0.00+0.87}_{-0.02-0.00-0.69}$ | 0.7 | 0.32 | 1.1 | 0.2 | 0.46 | 7.7 |
| $10^{-3} \times \mathcal{B}r(B_c^+ \rightarrow \eta_c(2S)\mu^+\nu_\mu)$ | $0.91^{+0.02+0.00+0.87}_{-0.02-0.00-0.69}$ | — | — | — | — | — | — |
| $10^{-5} \times \mathcal{B}r(B_c^+ \rightarrow \eta_c(2S)\tau^+\nu_\tau)$ | $8.22^{+0.14+0.02+7.37}_{-0.14-0.02-6.52}$ | — | — | 8.1 | — | 1.3 | 53 |
| $10^{-3} \times \mathcal{B}r(B_c^+ \rightarrow \eta_c(3S)e^+\nu_e)$ | $0.33^{+0.01+0.00+0.11}_{-0.01-0.00-0.11}$ | — | 0.0055 | 0.19 | — | — | 1.4 |
| $10^{-3} \times \mathcal{B}r(B_c^+ \rightarrow \eta_c(3S)\mu^+\nu_\mu)$ | $0.33^{+0.01+0.00+0.11}_{-0.01-0.00-0.11}$ | — | — | — | — | — | — |
| $10^{-5} \times \mathcal{B}r(B_c^+ \rightarrow \eta_c(3S)\tau^+\nu_\tau)$ | $0.39^{+0.01+0.00+0.13}_{-0.01-0.00-0.12}$ | — | 0.0005 | 0.57 | — | — | 0.19 |
| $10^{-3} \times \mathcal{B}r(B_c^+ \rightarrow \psi(2S)e^+\nu_e)$ | $2.34^{+0.04+0.04+0.09}_{-0.04-0.08-0.02}$ | 1 | 0.31 | — | 1.2 | 2.1 | 12 |
| $10^{-3} \times \mathcal{B}r(B_c^+ \rightarrow \psi(2S)\mu^+\nu_\mu)$ | $2.32^{+0.04+0.04+0.09}_{-0.04-0.08-0.02}$ | — | — | — | — | — | — |
| $10^{-5} \times \mathcal{B}r(B_c^+ \rightarrow \psi(2S)\tau^+\nu_\tau)$ | $15.89^{+0.28+0.06+0.09}_{-0.28-0.01-0.20}$ | — | — | — | — | 15 | 84 |
| $10^{-3} \times \mathcal{B}r(B_c^+ \rightarrow \psi(3S)e^+\nu_e)$ | $0.73^{+0.01+0.00+0.05}_{-0.01-0.00-0.05}$ | — | 0.0057 | — | — | — | 0.36 |
| $10^{-3} \times \mathcal{B}r(B_c^+ \rightarrow \psi(3S)\mu^+\nu_\mu)$ | $0.72^{+0.01+0.00+0.05}_{-0.01-0.00-0.05}$ | — | — | — | — | — | — |
| $10^{-5} \times \mathcal{B}r(B_c^+ \rightarrow \psi(3S)\tau^+\nu_\tau)$ | $0.58^{+0.01+0.00+0.03}_{-0.01-0.01-0.02}$ | — | 0.0036 | — | — | — | 0.038 |

The branching ratios of the semileptonic B_c decays to the radially excited charmonium states are shown in Tab. V, together with the results obtained in other approaches for comparison. The uncertainties are the same with those shown in Tab. IV. It is noticed that the large errors in the decays $B_c^+ \rightarrow \eta_c(2S)\ell^+\nu_\ell$ are induced by the decay constant $f_{\eta_c(2S)} = (243_{-111}^{+79})$ MeV [8]. For the decays $B_c^+ \rightarrow \eta_c(2S)\ell^+\nu_\ell, \psi(2S)\ell^+\nu_\ell$, their branching ratios are much smaller than the PQCD calculations [30]. Our predictions are consistent with the results given by the BS equation [18], the light-cone QCD sum rules [23] and the ISGW2 quark model [29]. Although the results for the semileptonic B_c decays to the ground state charmonia given by the relativistic quark model [20, 21] are appropriate, those for the semileptonic B_c decays to the radially excited charmonium states given by such approach seem to be too small. The branching ratios of these semileptonic decays show a clear hierarchical relationship,

$$\mathcal{B}r(B_c \rightarrow \eta_c(3S)\ell\nu_\ell) < \mathcal{B}r(B_c \rightarrow \eta_c(2S)\ell\nu_\ell) < \mathcal{B}r(B_c \rightarrow \eta_c(1S)\ell\nu_\ell), \quad (26)$$

$$\mathcal{B}r(B_c \rightarrow \psi(3S)\ell\nu_\ell) < \mathcal{B}r(B_c \rightarrow \psi(2S)\ell\nu_\ell) < \mathcal{B}r(B_c \rightarrow \psi(1S)\ell\nu_\ell). \quad (27)$$

The main reason is that the relationships $m_{\eta_c(1S)} < m_{\eta_c(2S)} < m_{\eta_c(3S)}$ and $m_{\psi(1S)} < m_{\psi(2S)} < m_{\psi(3S)}$ lead to the phase spaces of the final states decrease with the increasing of the radial quantum number n .

Similar with $R_{J/\Psi}$, it is useful to define the ratios of the branching ratios for the B_c decays to the radially excited charmonia, where the uncertainties induced by the model calculations and the CKM matrix elements can be cancelled,

$$R_{\psi(nS)} = \frac{\mathcal{B}r(B_c^+ \rightarrow \psi(nS)\tau^+\nu_\tau)}{\mathcal{B}r(B_c^+ \rightarrow \psi(nS)\mu^+\nu_\mu)}, \quad R_{\eta_c(nS)} = \frac{\mathcal{B}r(B_c^+ \rightarrow \eta_c(nS)\tau^+\nu_\tau)}{\mathcal{B}r(B_c^+ \rightarrow \eta_c(nS)\mu^+\nu_\mu)}, \quad (28)$$

where $n = 2, 3$. Our predictions R_X with $X = \eta_c(1S, 2S, 3S), \psi(1S, 2S, 3S)$ are collected in Tab. VI, together with the results obtained in other approaches for comparison. Obviously, it shows a clear hierarchical relationship,

$$R_{\psi(3S)} < R_{\psi(2S)} < R_{J/\Psi}, \quad R_{\eta_c(3S)} < R_{\eta_c(2S)} < R_{\eta_c(1S)}. \quad (29)$$

From Tab. VI, one can find that our predictions for these R values are comparable to other SM calculations. If the departures of the SM predictions for $R_{\psi(2S,3S)}$ and $R_{\eta_c(1S,2S,3S)}$ from the experimental data can be detected, it will further highlight the puzzle in flavor physics and the failure of lepton flavour universality hinted in the $R_{J/\Psi}$ measurement [13]. As our predictions for the branching ratios of these semileptonic B_c decays to the radially excited charmonia are larger than 10^{-6} , which can be measured in the future High-luminosity LHC (HL-LHC) and High-energy LHC (HE-LHC) experiments [42]. Then, the semileptonic B_c decays to the ground and excited charmonia will provide a more complete research area.

TABLE VI: The values of ratios R_X with $X = \eta_c(1S, 2S, 3S), \psi(1S, 2S, 3S)$.

| Ratio | This work | [36] | [22] | [19] | [31] | [20, 21] | [32] | [35] | [23] | [29] |
|------------------|---------------------|-------|------|--------|------|----------|--------|------|------|-------|
| R_{η_c} | 0.29 ± 0.02 | — | 0.27 | — | 0.31 | — | — | 0.25 | — | — |
| $R_{\eta_c(2S)}$ | 0.09 ± 0.12 | 0.14 | — | 0.054 | — | — | 0.069 | — | 0.74 | 0.028 |
| $R_{\eta_c(3S)}$ | 0.012 ± 0.006 | 0.021 | — | 0.010 | — | 0.0010 | 0.0014 | — | 0.03 | — |
| $R_{J/\psi}$ | 0.25 ± 0.04 | — | 0.24 | — | 0.29 | — | — | 0.24 | — | — |
| $R_{\psi(2S)}$ | 0.068 ± 0.003 | 0.085 | — | 0.51 | — | — | 0.070 | — | — | 0.071 |
| $R_{\psi(3S)}$ | 0.0081 ± 0.0007 | 0.078 | — | 0.0092 | — | 0.0063 | 0.0011 | — | — | — |

In order to investigate the impact of the lepton masses and provide more detailed physical picture for the semilepton B_c decays beyond the branching ratio, we also define another two physical observations that can be measured by experiments: the longitudinal polarization fraction f_L and the forward-backward asymmetry A_{FB} . These two physical quantities are sensitive to some kinds of new physics [43–47], so their values are helpful to test the SM and different NP scenarios. Meanwhile, the calculations of these two quantities may provide

new clues to understand the ratio $R_{J/\Psi}$ puzzle. We expect that these physical observables can be measured by the future LHCb experiments and it is helpful to clarify disputation from the different theoretical approaches. From the numerical results listed in Tab. VII and Tab. IX, the following points can be found:

TABLE VII: The longitudinal polarization fractions f_L (in%) for the decays $B_c^+ \rightarrow \eta_c(1S, 2S, 3S)\ell^+\nu_\ell$, $B_c^+ \rightarrow \psi(1S, 2S, 3S)\ell^+\nu_\ell$. The uncertainties are the same with those given in Table IV.

| Decay modes | $B_c^+ \rightarrow J/\psi e^+\nu_e$ | $B_c^+ \rightarrow J/\psi \mu^+\nu_\mu$ | $B_c^+ \rightarrow J/\psi \tau^+\nu_\tau$ |
|-------------|--------------------------------------|--|--|
| This work | $50.9^{+0.9+2.9+5.5}_{-0.9-4.6-5.1}$ | $50.9^{+0.9+3.0+5.7}_{-0.9-4.7-5.2}$ | $43.8^{+0.8+3.6+5.6}_{-0.8-4.7-5.1}$ |
| [30] | 33 | 33 | 39 |
| [51] | 44 | 44 | 40 |
| [52] | 51 | 51 | 45 |
| Decay modes | $B_c^+ \rightarrow \psi(2S)e^+\nu_e$ | $B_c^+ \rightarrow \psi(2S)\mu^+\nu_\mu$ | $B_c^+ \rightarrow \psi(2S)\tau^+\nu_\tau$ |
| This work | $59.2^{+1.0+0.1+0.1}_{-1.0-0.1-0.2}$ | $59.2^{+1.0+0.1+0.1}_{-1.0-0.1-0.2}$ | $44.6^{+0.8+0.1+0.2}_{-0.8-0.3-0.3}$ |
| [30] | 46 | 46 | 41 |
| Decay modes | $B_c^+ \rightarrow \psi(3S)e^+\nu_e$ | $B_c^+ \rightarrow \psi(3S)\mu^+\nu_\mu$ | $B_c^+ \rightarrow \psi(3S)\tau^+\nu_\tau$ |
| This work | $57.9^{+1.0+0.2+4.0}_{-1.0-0.1-4.1}$ | $57.9^{+1.0+0.2+4.0}_{-1.0-0.1-4.1}$ | $40.5^{+0.7+0.1+3.2}_{-0.7-0.2-3.1}$ |
| [30] | 54 | 54 | 31 |

(1) From Eqs.(13)-(16), we find that the longitudinal polarization fractions f_L of the decays $B_c^+ \rightarrow J/\psi\ell^+\nu_\ell$ decrease with the m_ℓ increasing although such trend is mild, that is

$$f_L(B_c^+ \rightarrow J/\psi e^+\nu_e) \approx f_L(B_c^+ \rightarrow J/\psi \mu^+\nu_\mu) > f_L(B_c^+ \rightarrow J/\psi \tau^+\nu_\tau), \quad (30)$$

which is support by our predictions shown in Tab. VII. Certainly, this rule can also be applied to the decays $B_c^+ \rightarrow \psi(2S, 3S)\ell^+\nu_\ell$.

TABLE VIII: Partial branching ratios and longitudinal polarization fraction f_L (in%) for the decays $B_c^+ \rightarrow \eta_c(1S, 2S, 3S)\ell^+\nu_\ell$, $B_c^+ \rightarrow \psi(1S, 2S, 3S)\ell^+\nu_\ell$ in Region 1 and Region 2.

| Observables | Region 1 | Region 2 | Observables | Region 1 | Region 2 | Observables | Region 1 | Region 2 |
|---|-----------------------|-----------------------|---|-----------------------|-----------------------|---|-----------------------|------------------------|
| $Br(B_c^+ \rightarrow J/\psi e^+\nu_e)$ | 0.71×10^{-2} | 0.89×10^{-2} | $Br(B_c^+ \rightarrow J/\psi \mu^+\nu_\mu)$ | 0.71×10^{-2} | 0.88×10^{-2} | $Br(B_c^+ \rightarrow J/\psi \tau^+\nu_\tau)$ | 0.13×10^{-2} | 0.27×10^{-2} |
| $f_L(B_c^+ \rightarrow J/\psi e^+\nu_e)$ | 64.5 | 40.1 | $f_L(B_c^+ \rightarrow J/\psi \mu^+\nu_\mu)$ | 64.5 | 40.1 | $f_L(B_c^+ \rightarrow J/\psi \tau^+\nu_\tau)$ | 53.9 | 40.1 |
| $Br(B_c^+ \rightarrow \psi(2S)e^+\nu_e)$ | 1.33×10^{-3} | 1.01×10^{-3} | $Br(B_c^+ \rightarrow \psi(2S)\mu^+\nu_\mu)$ | 1.31×10^{-3} | 1.01×10^{-3} | $Br(B_c^+ \rightarrow \psi(2S)\tau^+\nu_\tau)$ | 5.33×10^{-5} | 10.55×10^{-5} |
| $f_L(B_c^+ \rightarrow \psi(2S)e^+\nu_e)$ | 71.2 | 43.4 | $f_L(B_c^+ \rightarrow \psi(2S)\mu^+\nu_\mu)$ | 71.2 | 43.5 | $f_L(B_c^+ \rightarrow \psi(2S)\tau^+\nu_\tau)$ | 52.4 | 40.7 |
| $Br(B_c^+ \rightarrow \psi(3S)e^+\nu_e)$ | 0.40×10^{-3} | 0.33×10^{-3} | $Br(B_c^+ \rightarrow \psi(3S)\mu^+\nu_\mu)$ | 0.40×10^{-3} | 0.33×10^{-3} | $Br(B_c^+ \rightarrow \psi(3S)\tau^+\nu_\tau)$ | 0.16×10^{-5} | 0.42×10^{-5} |
| $f_L(B_c^+ \rightarrow \psi(3S)e^+\nu_e)$ | 70.2 | 42.8 | $f_L(B_c^+ \rightarrow \psi(3S)\mu^+\nu_\mu)$ | 70.2 | 42.9 | $f_L(B_c^+ \rightarrow \psi(3S)\tau^+\nu_\tau)$ | 45.7 | 38.1 |

In order to investigate the dependences of the polarizations on the different q^2 , we calculate the longitudinal polarization fractions by dividing the full energy region into two regions for each decay, which are listed in Tab. VIII, together with the partial branching ratios, where Region 1 is defined as $m_\ell^2 < q^2 < \frac{(m_{B_c} - m_{\psi(nS)})^2 + m_\ell^2}{2}$ and Region 2 is $\frac{(m_{B_c} - m_{\psi(nS)})^2 + m_\ell^2}{2} < q^2 < (m_{B_c} - m_{\psi(nS)})^2$ with $n = 1, 2, 3$. From Tab. VIII, one can find that in Region 1 the longitudinal polarizations dominate the branching ratios for the decays with e and μ involved, while the longitudinal and transverse polarizations for the decay channels involving τ are comparable in Region 1. It is interesting that for all the considered decays the transverse polarizations are dominant in Region 2. These results can be tested by the future LHCb experiments.

TABLE IX: The forward-backward asymmetries A_{FB} for the decays $B_c^+ \rightarrow \eta_c(1S, 2S, 3S)\ell^+\nu_\ell$ and $B_c^+ \rightarrow \psi(1S, 2S, 3S)\ell^+\nu_\ell$.

| | | | |
|-------------|---|---|--|
| Decay modes | $B_c^+ \rightarrow \eta_c e^+ \nu_e$ | $B_c^+ \rightarrow \eta_c \mu^+ \nu_\mu$ | $B_c^+ \rightarrow \eta_c \tau^+ \nu_\tau$ |
| This work | $(3.93_{-0.07-0.00-0.01}^{+0.07+0.00+0.14}) \times 10^{-7}$ | $0.015_{-0.000-0.000-0.000}^{+0.000+0.000+0.001}$ | $0.36_{-0.01-0.01-0.01}^{+0.01+0.01+0.02}$ |
| [51] | -8.6×10^{-7} | -0.012 | -0.35 |
| [53] | -2.049×10^{-7} | - | 0.357 |
| [54] | - | - | 0.364 |
| Decay modes | $B_c^+ \rightarrow \eta_c(2S) e^+ \nu_e$ | $B_c^+ \rightarrow \eta_c(2S) \mu^+ \nu_\mu$ | $B_c^+ \rightarrow \eta_c(2S) \tau^+ \nu_\tau$ |
| This work | $(6.96_{-0.12-0.00-5.17}^{+0.12+0.00+5.69}) \times 10^{-7}$ | $0.023_{-0.000-0.000-0.017}^{+0.000+0.000+0.019}$ | $0.30_{-0.01-0.00-0.24}^{+0.01+0.00+0.28}$ |
| [36] | 5.75×10^{-7} | - | 0.384 |
| Decay modes | $B_c^+ \rightarrow \eta_c(3S) e^+ \nu_e$ | $B_c^+ \rightarrow \eta_c(3S) \mu^+ \nu_\mu$ | $B_c^+ \rightarrow \eta_c(3S) \tau^+ \nu_\tau$ |
| This work | $(9.00_{-0.16-0.00-2.88}^{+0.16+0.00+2.77}) \times 10^{-7}$ | $0.028_{-0.000-0.000-0.009}^{+0.000+0.000+0.009}$ | $0.33_{-0.01-0.00-0.12}^{+0.01+0.00+0.14}$ |
| [36] | 10.5×10^{-7} | - | 0.367 |
| Decay modes | $B_c^+ \rightarrow J/\psi e^+ \nu_e$ | $B_c^+ \rightarrow J/\psi \mu^+ \nu_\mu$ | $B_c^+ \rightarrow J/\psi \tau^+ \nu_\tau$ |
| This work | $-0.21_{-0.00-0.02-0.02}^{+0.00+0.02+0.02}$ | $-0.21_{-0.00-0.02-0.02}^{+0.00+0.02+0.02}$ | $-0.14_{-0.00-0.01-0.02}^{+0.00+0.01+0.02}$ |
| [51] | -0.19 | -0.19 | -0.23 |
| [53] | 0.18 | - | -0.255 |
| [54] | - | - | -0.042 |
| Decay modes | $B_c^+ \rightarrow \psi(2S) e^+ \nu_e$ | $B_c^+ \rightarrow \psi(2S) \mu^+ \nu_\mu$ | $B_c^+ \rightarrow \psi(2S) \tau^+ \nu_\tau$ |
| This work | $-0.16_{-0.00-0.00-0.01}^{+0.00+0.00+0.00}$ | $-0.16_{-0.00-0.00-0.01}^{+0.00+0.00+0.00}$ | $-0.093_{-0.002-0.000-0.003}^{+0.002+0.000+0.014}$ |
| [36] | -0.246 | - | -0.214 |
| Decay modes | $B_c^+ \rightarrow \psi(3S) e^+ \nu_e$ | $B_c^+ \rightarrow \psi(3S) \mu^+ \nu_\mu$ | $B_c^+ \rightarrow \psi(3S) \tau^+ \nu_\tau$ |
| This work | $-0.14_{-0.00-0.00-0.01}^{+0.00+0.00+0.01}$ | $-0.14_{-0.00-0.00-0.01}^{+0.00+0.00+0.01}$ | $-0.048_{-0.001-0.008-0.003}^{+0.001+0.009+0.014}$ |
| [36] | -0.155 | - | -0.144 |

(2) From Tab. IX, we find that the ratios of the forward-backward asymmetries A_{FB}

between the different semileptonic decays associated with the $B_c \rightarrow \eta_c(nS)$ transitions have the following rules: $A_{FB}^\mu/A_{FB}^e = (3 \sim 4) \times 10^4$ and $A_{FB}^\tau/A_{FB}^e > 1 \times 10^5$. It is because that A_{FB} for $B_c \rightarrow \eta_c(nS)$ transitions are proportional to the square of the lepton mass shown in Eqs.(17)-(18). Undoubtedly, the effect of lepton mass can be well checked in such decay modes with the pseudoscalar mesons involved in the final states. As to the $B_c \rightarrow \psi(nS)$ transitions, the values of the forward-backward asymmetries A_{FB}^μ are almost equal to those of A_{FB}^e , while the values of A_{FB}^τ are smaller than those of $A_{FB}^{e(\mu)}$. It is noticed that dominant contribution to the A_{FB} for the $B_c \rightarrow \psi(nS)$ transitions arises from the term proportional to $(H_+^2 - H_-^2)$ in Eq. (19).

In Figs. 2 and 3, we display the q^2 -dependences of the differential decay rates $d\Gamma_{(L)}/dq^2$ and the forward-backward asymmetries A_{FB} , respectively. It can be observed that the values of $d\Gamma_{(L)}/dq^2$ and A_{FB} coincide with 0 at the zero recoil point ($q^2 = q_{max}^2$) since the coefficient $\lambda(q^2) = \lambda(m_{B_c}^2, m_{\eta_c/\psi}^2, q^2)$ shown in Eqs. (10)-(19) at the same zero recoil point being equal to 0. Furthermore, it is very different for the q^2 dependences of the differential decay rates from the longitudinal polarization $d\Gamma_L/dq^2$ between the decays $B_c^+ \rightarrow J/\Psi \ell'^+ \nu_{\ell'}$ and $B_c^+ \rightarrow \psi(2S, 3S) \ell'^+ \nu_{\ell'}$.

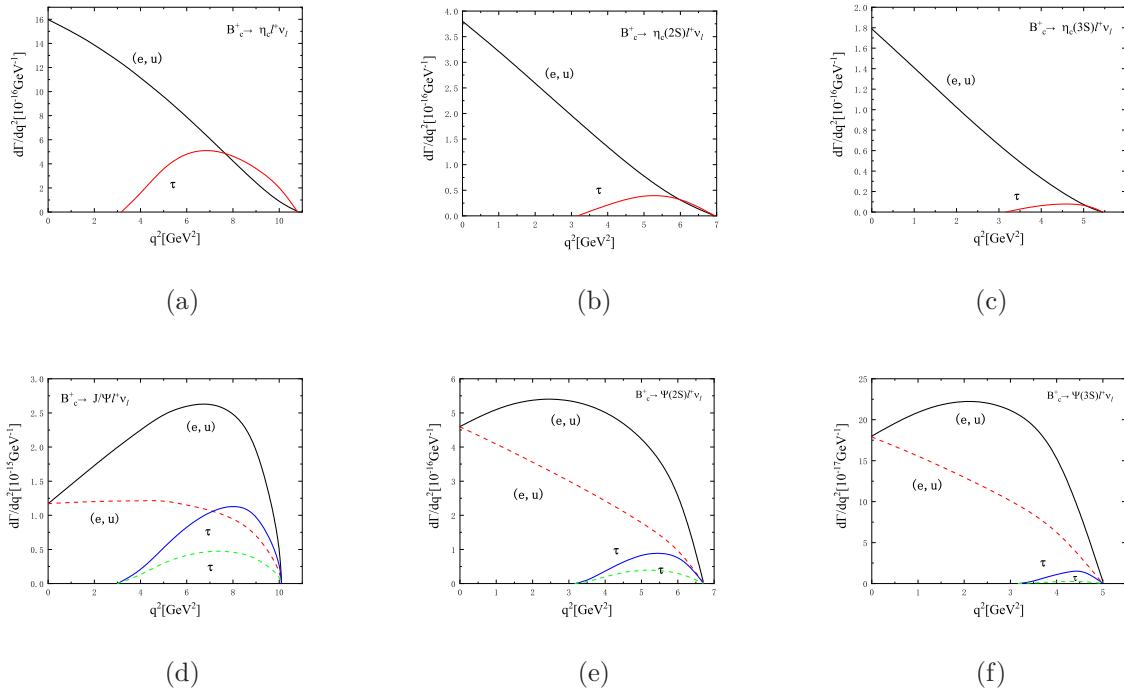


FIG. 2: The q^2 dependences of the differential decay rates $d\Gamma/dq^2$ (solid lines) and $d\Gamma_L/dq^2$ (dashed lines) with L representing the contribution from the longitudinal polarization.

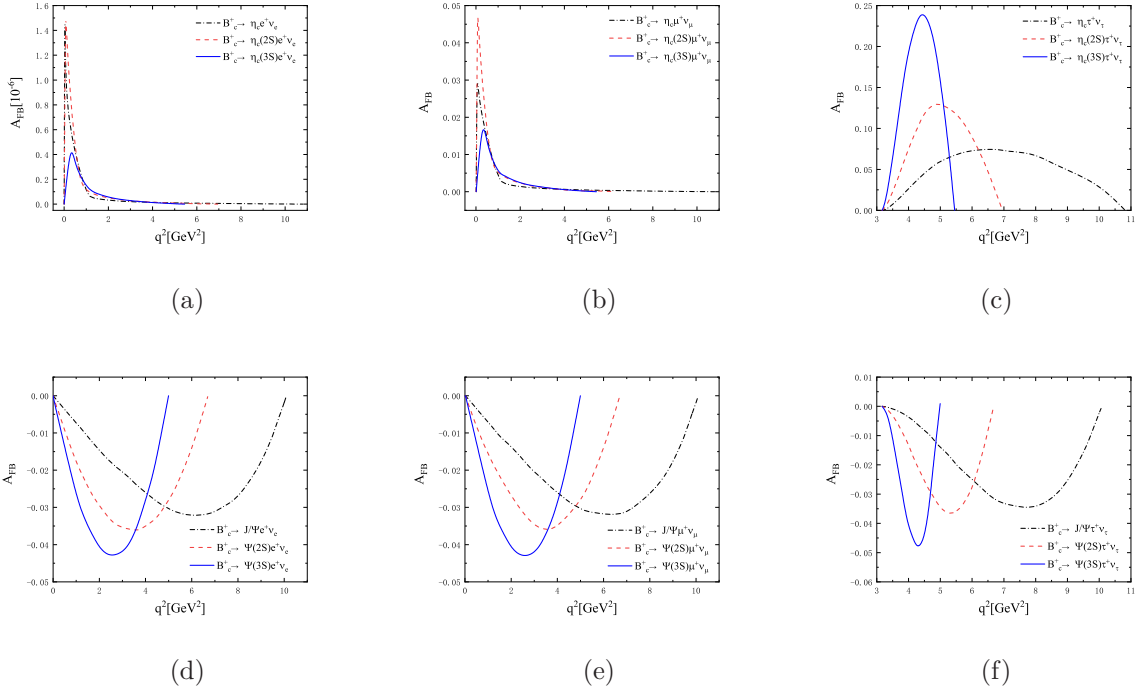


FIG. 3: The q^2 dependences of the forward-backward asymmetries A_{FB} for the decays $B_c \rightarrow \eta_c(1S, 2S, 3S)\ell^+\nu_\ell$ and $B_c \rightarrow \psi(1S, 2S, 3S)\ell^+\nu_\ell$.

Similarly, we also analysis the semileptonic decays $B_c^+ \rightarrow X(3872)\ell^+\nu_\ell$ by assuming the $X(3872)$ as a regular $c\bar{c}$ charmonium state. The branching ratios, the longitudinal polarization fractions f_L and the forward-backward asymmetries A_{FB} are listed in Tab. X. One can find that $\mathcal{B}r(B_c^+ \rightarrow X(3872)\tau^+\nu_\tau)$ is only about one twenty-fifth of $\mathcal{B}r(B_c^+ \rightarrow X(3872)\ell^+\nu_\ell)$ due to the narrower phase space of the final states with the τ lepton involved. Obviously, our predictions are consistent with those given in the generalized factorization approach (GFA) [48], while are about $7 \sim 9$ times smaller than those in the QCDSR approach [23]. The ratio R_X is

$$R_X = \frac{\mathcal{B}r(B_c^+ \rightarrow X(3872)\tau^+\nu_\tau)}{\mathcal{B}r(B_c^+ \rightarrow X(3872)\mu^+\nu_\mu)} = 0.040 \pm 0.006, \quad (31)$$

which is consistent with the value $R_X = 0.048$ given by the GFA and QCDSR. There exists significant difference between $B_c^+ \rightarrow X(3872)\ell^+\nu_\ell$ and $B_c^+ \rightarrow J/\psi\ell^+\nu_\ell$ with in the polarization fractions: the transverse polarization is dominant in the former, while the longitudinal and transverse polarizations are comparable in the latter. For the decays $B_c^+ \rightarrow X(3872)\tau^+\nu_\tau$ and $B_c^+ \rightarrow J/\Psi\tau^+\nu_\tau$, both of them are dominated by the transverse polarization. The forward-backward asymmetries A_{FB} for the decays $B_c^+ \rightarrow X(3872)\ell^+\nu_\ell$ are about two times larger in magnitude than those for the channels $B_c^+ \rightarrow J/\Psi\ell^+\nu_\ell$. As to

TABLE X: Branching ratios, the longitudinal polarization fractions f_L and the forward-backward asymmetries A_{FB} for the semileptonic decays $B_c^+ \rightarrow X(3872)\ell^+\nu_\ell$.

| Decay Modes | $\mathcal{B}r(10^{-4})$ | | | $f_L(\%)$ | A_{FB} |
|---|--|------|------|--------------------------------------|---|
| | This work | [48] | [23] | | |
| $B_c^+ \rightarrow X(3872)e^+\nu_e$ | $9.27^{+0.16+0.01+0.58}_{-0.16-0.22-0.89}$ | 13.5 | 67 | $36.7^{+0.6+0.0+2.5}_{-0.6-0.1-1.3}$ | $-0.45^{+0.01+0.00+0.07}_{-0.01-0.00-0.05}$ |
| $B_c^+ \rightarrow X(3872)\mu^+\nu_\mu$ | $9.20^{+0.16+0.01+0.57}_{-0.16-0.21-0.89}$ | 13.5 | — | $36.7^{+0.6+0.0+2.5}_{-0.6-0.0-1.3}$ | $-0.44^{+0.01+0.00+0.07}_{-0.01-0.00-0.05}$ |
| $B_c^+ \rightarrow X(3872)\tau^+\nu_\tau$ | $0.37^{+0.01+0.00+0.04}_{-0.01-0.00-0.04}$ | 0.65 | 3.2 | $31.9^{+0.6+0.1+2.6}_{-0.6-0.5-3.1}$ | $-0.28^{+0.01+0.00+0.05}_{-0.01-0.00-0.04}$ |

the partial branching ratios and longitudinal polarization fractions in Region 1 and Region 2 defined in the previous section are given in Tab. XI, where the transverse polarizations are dominant in both cases. It is evident that the dominant contributions arise from the transverse polarizations whether in Region 1, Region 2, or the entire physical region. All of these values are meaningful to determining the inner structure of X(3872) by comparing with the future experimental measurements.

In Fig. 4, we plot the q^2 dependences of the differential decay rates $d\Gamma_{(L)}/dq^2$ with L referring the longitudinal polarization and the forward-backward asymmetries A_{FB} for the decays $B_c^+ \rightarrow X(3872)\ell^+\nu_\ell$, where it is similar in character to the cases of $B_c^+ \rightarrow \psi(nS)\ell^+\nu_\ell$, that is the values of $d\Gamma_{(L)}/dq^2$ and A_{FB} are coincide with 0 at the zero recoil point ($q^2 = q_{max}^2$). Furthermore, the differential decay rate from the transverse polarization $d\Gamma_T/dq^2(B_c^+ \rightarrow X(3872)\ell^+\nu_\ell)$ is much more sensitive to the change of q^2 compared with that from the longitudinal polarization $d\Gamma_L/dq^2(B_c^+ \rightarrow X(3872)\ell^+\nu_\ell)$.

TABLE XI: The partial branching ratios and longitudinal polarization fraction f_L (in%) for the decays $B_c^+ \rightarrow X(3872)\ell^+\nu_\ell$.

| Observables | Region 1 | Region 2 | Observables | Region 1 | Region 2 | Observables | Region 1 | Region 2 |
|---|-----------------------|-----------------------|---|-----------------------|-----------------------|---|-----------------------|-----------------------|
| $\mathcal{B}r(B_c^+ \rightarrow X(3872)e^+\nu_e)$ | 0.47×10^{-3} | 0.46×10^{-3} | $\mathcal{B}r(B_c^+ \rightarrow X(3872)\mu^+\nu_\mu)$ | 0.46×10^{-3} | 0.46×10^{-3} | $\mathcal{B}r(B_c^+ \rightarrow X(3872)\tau^+\nu_\tau)$ | 1.15×10^{-5} | 2.58×10^{-5} |
| $f_L(B_c^+ \rightarrow X(3872)e^+\nu_e)$ | 43.4 | 29.9 | $f_L(B_c^+ \rightarrow X(3872)\mu^+\nu_\mu)$ | 43.4 | 29.9 | $f_L(B_c^+ \rightarrow X(3872)\tau^+\nu_\tau)$ | 32.3 | 31.7 |

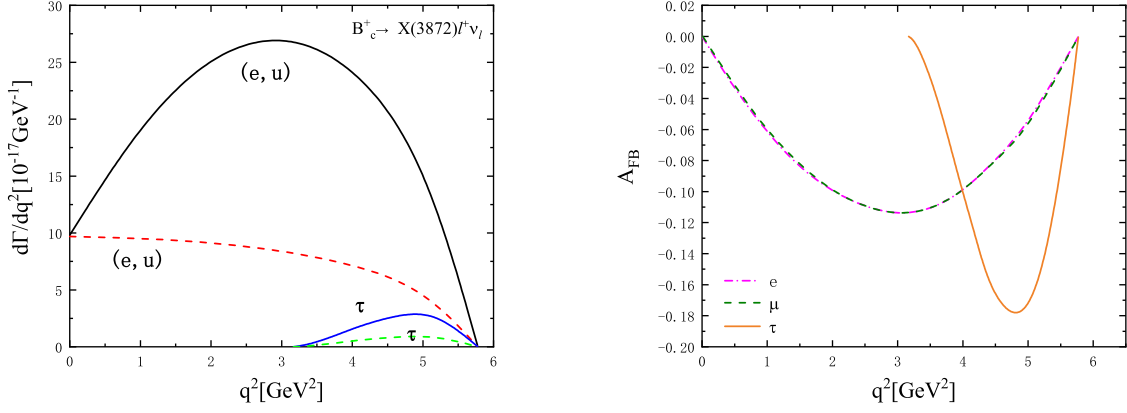


FIG. 4: The q^2 dependences of the differential decay rates $d\Gamma/dq^2$ (solid lines) and $d\Gamma_L/dq^2$ (dashed lines) are shown on the left pannel and the q^2 dependences of the forward-backward asymmetries A_{FB} for the decays $B_c^+ \rightarrow X(3872)\ell^+\nu_\ell$ are shown on the right pannel.

IV. SUMMARY

In this work, we investigated the exclusive semileptonic B_c decays to $\eta_c(1S, 2S, 3S), \psi(1S, 2S, 3S)$ and $X(3872)$ in the CLFQM. Using the helicity amplitudes combined via the form factors, we calculated the branching ratios, the longitudinal polarization fractions f_L and the forward-backward asymmetries A_{FB} for these semileptonic B_c decays. From the numerical results, we found the following points:

1. Compared the branching ratios of these semileptonic decays, it shows a clear hierarchical relationship,

$$\mathcal{B}r(B_c \rightarrow X(3S)\ell\nu_\ell) < \mathcal{B}r(B_c \rightarrow X(2S)\ell\nu_\ell) < \mathcal{B}r(B_c \rightarrow X(1S)\ell\nu_\ell), \quad (32)$$

where $X = \eta_c, \psi$.

2. The ratios $R_X = \frac{\mathcal{B}r(B_c^+ \rightarrow X\tau^+\nu_\tau)}{\mathcal{B}r(B_c^+ \rightarrow X\mu^+\nu_\mu)}$ are predicted as

$$R_{J/\psi} = 0.25 \pm 0.04, R_{\psi(2S)} = 0.068 \pm 0.003, R_{\psi(3S)} = 0.0081 \pm 0.0007, \quad (33)$$

$$R_{\eta_c} = 0.29 \pm 0.02, R_{\eta_c(2S)} = 0.09 \pm 0.12, R_{\eta_c(3S)} = 0.012 \pm 0.006, \quad (34)$$

$$R_{X(3872)} = 0.040 \pm 0.006. \quad (35)$$

3. The longitudinal polarization fractions f_L of the decays $B_c^+ \rightarrow \psi\ell^+\nu_\ell$ have the following rules

$$f_L(B_c^+ \rightarrow \psi(nS)e^+\nu_e) \approx f_L(B_c^+ \rightarrow \psi(nS)\mu^+\nu_\mu) > f_L(B_c^+ \rightarrow \psi(nS)\tau^+\nu_\tau). \quad (36)$$

The longitudinal polarization dominates the branching ratios for the decays with e and μ involved, while the transverse polarization is dominant for the decays with τ involved. It is different for the decays $B_c^+ \rightarrow X(3872)\ell^+\nu_\ell$, where the transverse polarization is dominant in any case.

4. The ratios of the forward-backward asymmetries A_{FB} between the different semileptonic decays associated with the $B_c \rightarrow \eta_c(nS)$ transitions are given as

$$\frac{A_{FB}^\mu}{A_{FB}^e} = (3 \sim 4) \times 10^4, \quad \frac{A_{FB}^\tau}{A_{FB}^e} > 1 \times 10^5. \quad (37)$$

While the forward-backward asymmetries A_{FB} for the decays $B_c^+ \rightarrow \psi(nS)\ell^+\nu_\ell$ and $B_c^+ \rightarrow X(3872)\ell^+\nu_\ell$ become minus in sign, the differences between these values A_{FB}^ℓ are small and less than 3 times.

5. Our predictions are helpful to test the standard model and different new physics scenarios. Certainly, the values correlated with the $X(3872)$ are also meaningful to determining the inner structure of the $X(3872)$ by comparing with the future experimental measurements.

Acknowledgment

This work is partly supported by the National Natural Science Foundation of China under Grant No. 11347030, the Program of Science and Technology Innovation Talents in Universities of Henan Province 14HASTIT037, as well as the Natural Science Foundation of Henan Province under Grant No. 232300420116.

Appendix A: Some specific rules under the p^- intergration

When performing the integraion, we need to include the zero-mode contributions. It amounts to performing the integration in a proper way in the CLFQM. Specifically we use the following rules given in Refs. [7, 11]

$$\hat{p}'_{1\mu} \doteq P_\mu A_1^{(1)} + q_\mu A_2^{(1)}, \quad (A1)$$

$$\hat{p}'_{1\mu}\hat{p}'_{1\nu} \doteq g_{\mu\nu}A_1^{(2)} + P_\mu P_\nu A_2^{(2)} + (P_\mu q_\nu + q_\mu P_\nu) A_3^{(2)} + q_\mu q_\nu A_4^{(2)}, \quad (A2)$$

$$Z_2 = \hat{N}'_1 + m_1'^2 - m_2^2 + (1 - 2x_1) M'^2 + (q^2 + q \cdot P) \frac{p'_\perp \cdot q_\perp}{q^2}, \quad (A3)$$

$$A_1^{(1)} = \frac{x_1}{2}, \quad A_2^{(1)} = A_1^{(1)} - \frac{p'_\perp \cdot q_\perp}{q^2}, \quad A_3^{(2)} = A_1^{(1)} A_2^{(1)}, \quad (A4)$$

$$A_4^{(2)} = \left(A_2^{(1)}\right)^2 - \frac{1}{q^2} A_1^{(2)}, \quad A_1^{(2)} = -p_\perp'^2 - \frac{(p'_\perp \cdot q_\perp)^2}{q^2}, \quad A_2^{(2)} = \left(A_1^{(1)}\right)^2. \quad (A5)$$

Appendix B: EXPRESSIONS OF $B_c \rightarrow P, V, A$ FORM FACTORS

The following are the analytical expressions of the $B_c \rightarrow \eta_c(1S, 2S, 3S), \psi(1S, 2S, 3S), X(3872)$ transition form factors in the covariant light-front quark model

$$F_1^{B_c \eta_c}(q^2) = \frac{N_c}{16\pi^3} \int dx_2 d^2 p'_\perp \frac{h'_{B_c} h''_{\eta_c}}{x_2 \hat{N}'_1 \hat{N}''_1} [x_1 (M_0'^2 + M_0''^2) + x_2 q^2 - x_2 (m'_1 - m''_1)^2 - x_1 (m'_1 - m_2)^2 - x_1 (m''_1 - m_2)^2] \quad (B1)$$

$$F_0^{B_c \eta_c}(q^2) = F_1^{B_c \eta_c}(q^2) + \frac{q^2}{(q \cdot P)} \frac{N_c}{16\pi^3} \int dx_2 d^2 p'_\perp \frac{2h'_{B_c} h''_{\eta_c}}{x_2 \hat{N}'_1 \hat{N}''_1} \left\{ -x_1 x_2 M'^2 - p_\perp'^2 - m'_1 m_2 + (m''_1 - m_2)(x_2 m'_1 + x_1 m_2) + 2 \frac{q \cdot P}{q^2} \left(p_\perp'^2 + 2 \frac{(p'_\perp \cdot q_\perp)^2}{q^2} \right) + 2 \frac{(p'_\perp \cdot q_\perp)^2}{q^2} - \frac{p'_\perp \cdot q_\perp}{q^2} [M''^2 - x_2 (q^2 + q \cdot P) - (x_2 - x_1) M'^2 + 2x_1 M_0'^2 - 2(m'_1 - m_2)(m'_1 + m''_1)] \right\}, \quad (B2)$$

$$V^{B_c \psi}(q^2) = \frac{N_c (M' + M'')}{16\pi^3} \int dx_2 d^2 p'_\perp \frac{2h'_{B_c} h''_\psi}{x_2 \hat{N}'_1 \hat{N}''_1} \left\{ x_2 m'_1 + x_1 m_2 + (m'_1 - m''_1) \frac{p'_\perp \cdot q_\perp}{q^2} + \frac{2}{w'_\psi} \left[p_\perp'^2 + \frac{(p'_\perp \cdot q_\perp)^2}{q^2} \right] \right\}, \quad (B3)$$

$$A_1^{B_c \psi}(q^2) = -\frac{1}{M' + M''} \frac{N_c}{16\pi^3} \int dx_2 d^2 p'_\perp \frac{h'_{B_c} h''_\psi}{x_2 \hat{N}'_1 \hat{N}''_1} \left\{ 2x_1 (m_2 - m'_1) (M_0'^2 + M_0''^2) - 4x_1 m''_1 M_0'^2 + 2x_2 m'_1 q \cdot P + 2m_2 q^2 - 2x_1 m_2 (M'^2 + M''^2) + 2(m'_1 - m_2)(m'_1 + m''_1)^2 + 8(m'_1 - m_2) \times \left[p_\perp'^2 + \frac{(p'_\perp \cdot q_\perp)^2}{q^2} \right] + 2(m'_1 + m''_1)(q^2 + q \cdot P) \frac{p'_\perp \cdot q_\perp}{q^2} - 4 \frac{q^2 p_\perp'^2 + (p'_\perp \cdot q_\perp)^2}{q^2 w''_\psi} \times \left[2x_1 (M'^2 + M_0'^2) - q^2 - q \cdot P - 2(q^2 + q \cdot P) \frac{p'_\perp \cdot q_\perp}{q^2} - 2(m'_1 - m''_1)(m'_1 - m_2) \right] \right\}, \quad (B4)$$

$$A_2^{B_c \psi}(q^2) = \frac{N_c (M' + M'')}{16\pi^3} \int dx_2 d^2 p'_\perp \frac{2h'_{B_c} h''_\psi}{x_2 \hat{N}'_1 \hat{N}''_1} \left\{ (x_1 - x_2)(x_2 m'_1 + x_1 m_2) - \frac{p'_\perp \cdot q_\perp}{q^2} [2x_1 m_2 + m''_1 + (x_2 - x_1) m'_1] - 2 \frac{x_2 q^2 + p'_\perp \cdot q_\perp}{x_2 q^2 w''_\psi} [p'_\perp \cdot p''_\perp + (x_1 m_2 + x_2 m'_1)(x_1 m_2 - x_2 m''_1)] \right\}, \quad (B5)$$

$$A_0^{B_c \psi}(q^2) = \frac{M' + M''}{2M''} A_1^{B_c \psi}(q^2) - \frac{M' - M''}{2M''} A_2^{B_c \psi}(q^2) - \frac{q^2}{2M''} \frac{N_c}{16\pi^3} \int dx_2 d^2 p'_\perp \frac{h'_{B_c} h''_\psi}{x_2 \hat{N}'_1 \hat{N}''_1} \left\{ 2(2x_1 - 3)(x_2 m'_1 + x_1 m_2) - 8(m'_1 - m_2) \times \left[\frac{p_\perp'^2}{q^2} + 2 \frac{(p'_\perp \cdot q_\perp)^2}{q^4} \right] - [(14 - 12x_1) m'_1 - 2m''_1 - (8 - 12x_1) m_2] \frac{p'_\perp \cdot q_\perp}{q^2} + \frac{4}{w''_\psi} ([M'^2 + M''^2 - q^2 + 2(m'_1 - m_2)(m''_1 + m_2)] \times (A_3^{(2)} + A_4^{(2)} - A_2^{(1)}) + Z_2 (3A_2^{(1)} - 2A_4^{(2)} - 1) + \frac{1}{2} [x_1 (q^2 + q \cdot P) - 2M'^2 - 2p'_\perp \cdot q_\perp - 2m'_1 (m''_1 + m_2) - 2m_2 (m'_1 - m_2)] (A_1^{(1)} + A_2^{(1)} - 1) q \cdot P \left[\frac{p_\perp'^2}{q^2} + \frac{(p'_\perp \cdot q_\perp)^2}{q^4} \right] \times (4A_2^{(1)} - 3) \right\}, \quad (B6)$$

$$\begin{aligned}
A^{B_c X}(q^2) &= (M' - M'') \frac{N_c}{16\pi^3} \int dx_2 d^2 p'_\perp \frac{2h'_{B_c} h''_X}{x_2 \hat{N}'_1 \hat{N}''_1} \left\{ x_2 m'_1 + x_1 m_2 + (m'_1 + m''_1) \frac{p'_\perp \cdot q_\perp}{q^2} \right. \\
&\quad \left. + \frac{2}{w''_X} \left[p'^2_\perp + \frac{(p'_\perp \cdot q_\perp)^2}{q^2} \right] \right\}, \tag{B7}
\end{aligned}$$

$$\begin{aligned}
V_1^{B_c X}(q^2) &= -\frac{1}{M' - M''} \frac{N_c}{16\pi^3} \int dx_2 d^2 p'_\perp \frac{h'_{B_c} h''_X}{x_2 \hat{N}'_1 \hat{N}''_1} \left\{ 2x_1 (m_2 - m'_1) (M_0'^2 + M_0''^2) + 4x_1 m'_1 M_0'^2 \right. \\
&\quad + 2x_2 m'_1 q \cdot P + 2m_2 q^2 - 2x_1 m_2 (M'^2 + M''^2) + 2(m'_1 - m_2) (m'_1 - m''_1)^2 + 8(m'_1 - m_2) \\
&\quad \times \left[p'^2_\perp + \frac{(p'_\perp \cdot q_\perp)^2}{q^2} \right] + 2(m'_1 - m''_1) (q^2 + q \cdot P) \frac{p'_\perp \cdot q_\perp}{q^2} - 4 \frac{q^2 p'^2_\perp + (p'_\perp \cdot q_\perp)^2}{q^2 w''_X} \\
&\quad \left. \times \left[2x_1 (M'^2 + M_0'^2) - q^2 - q \cdot P - 2(q^2 + q \cdot P) \frac{p'_\perp \cdot q_\perp}{q^2} - 2(m'_1 + m''_1) (m'_1 - m_2) \right] \right\}, \tag{B8}
\end{aligned}$$

$$\begin{aligned}
V_2^{B_c X}(q^2) &= (M' - M'') \frac{N_c}{16\pi^3} \int dx_2 d^2 p'_\perp \frac{2h'_{B_c} h''_X}{x_2 \hat{N}'_1 \hat{N}''_1} \left\{ (x_1 - x_2) (x_2 m'_1 + x_1 m_2) - [2x_1 m_2 - m''_1 \right. \\
&\quad + (x_2 - x_1) m'_1] \times \frac{p'_\perp \cdot q_\perp}{q^2} - 2 \frac{x_2 q^2 + p'_\perp \cdot q_\perp}{x_2 q^2 w''_X} [p'_\perp \cdot p''_\perp + (x_1 m_2 + x_2 m'_1) \\
&\quad \left. \times (x_1 m_2 + x_2 m''_1)] \right\}, \tag{B9}
\end{aligned}$$

$$\begin{aligned}
V_0^{B_c X}(q^2) &= \frac{M' - M''}{2M''} V_1^{B_c X}(q^2) - \frac{M' + M''}{2M''} V_2^{B_c}(q^2) - \frac{q^2}{2M''} \frac{N_c}{16\pi^3} \int dx_2 d^2 p'_\perp \frac{h'_{B_c} h''_X}{x_2 \hat{N}'_1 \hat{N}''_1} \\
&\quad \times \left\{ 2(2x_1 - 3)(x_2 m'_1 + x_1 m_2) - 8(m'_1 - m_2) \left[\frac{p'^2_\perp}{q^2} + 2 \frac{(p'_\perp \cdot q_\perp)^2}{q^4} \right] - [(14 - 12x_1) m'_1 \right. \\
&\quad + 2m''_1 - (8 - 12x_1) m_2] \frac{p'_\perp \cdot q_\perp}{q^2} + \frac{4}{w''_X} ([M'^2 + M''^2 - q^2 + 2(m'_1 - m_2)(-m''_1 + m_2)] \\
&\quad \times (A_3^{(2)} + A_4^{(2)} - A_2^{(1)}) + Z_2 (3A_2^{(1)} - 2A_4^{(2)} - 1) + \frac{1}{2} [x_1 (q^2 + q \cdot P) - 2M'^2 - 2p'_\perp \cdot q_\perp \\
&\quad - 2m'_1 (-m''_1 + m_2) - 2m_2 (m'_1 - m_2)] (A_1^{(1)} + A_2^{(1)} - 1) \\
&\quad \left. \times q \cdot P \left[\frac{p'^2_\perp}{q^2} + \frac{(p'_\perp \cdot q_\perp)^2}{q^4} \right] (4A_2^{(1)} - 3) \right\}. \tag{B10}
\end{aligned}$$

-
- [1] M. V. Terentev, Sov. J. Nucl. Phys. **24**, 106 (1976) [Yad. Fiz. **24**, 207 (1976)].
- [2] V. B. Berestetsky and M. V. Terentev, Sov. J. Nucl. Phys. **25**, 347 (1977) [Yad. Fiz. **25**, 653 (1977)].
- [3] P. A. Dirac, Rev. Mod. Phys. **21**, 392 (1949).
- [4] W. Jaus, Phys. Rev. D **41**, 3394 (1990).
- [5] W. Jaus, Phys. Rev. D **44**, 2851 (1991).
- [6] H. M. Choi and C. R. Ji, Phys. Lett. B **460**, 461 (1999) [arXiv:hep-ph/9903496].
- [7] W. Jaus, Phys. Rev. D **60**, 054026 (1999).
- [8] Z. Q. Zhang, Z. J. Sun, Y. C. Zhao, Y. Y. Yang and Z. Y. Zhang, Eur. Phys. J. C **83**, 477 (2023) [arXiv:2301.11107 [hep-ph]].

- [9] W. Wang, Y. L. Shen and C. D. Lu, Phys. Rev. D **79**, 054012 (2009) [arXiv:0811.3748 [hep-ph]].
- [10] H. W. Ke, T. Liu and X. Q. Li, Phys. Rev. D **89**, 017501 (2014) [arXiv:1307.5925 [hep-ph]].
- [11] H. Y. Cheng, C. K. Chua and C. W. Hwang, Phys. Rev. D **69** (2004), 074025 [arXiv:hep-ph/0310359].
- [12] X. X. Wang, W. Wang and C. D. Lu, Phys. Rev. D **79**, 114018 (2009) [arXiv:0901.1934 [hep-ph]].
- [13] R. Aaij *et al.* [LHCb Collaboration], Phys. Rev. Lett. **120**, 121801 (2018) [arXiv:1711.05623 [hep-ex]].
- [14] T. D. Cohen, H. Lamm and R. F. Lebed, JHEP **09**, 168 (2018) [arXiv:1807.02730 [hep-ph]].
- [15] A. Issadykov and M. A. Ivanov, Phys. Lett. B **783**, 178 (2018) [arXiv:1804.00472 [hep-ph]].
- [16] C. F. Qiao and R. L. Zhu, Phys. Rev. D **87**, 014009 (2013) [arXiv:1208.5916 [hep-ph]].
- [17] C. F. Qiao, P. Sun, D. Yang and R. L. Zhu, Phys. Rev. D **89**, 034008 (2014) [arXiv:1209.5859 [hep-ph]].
- [18] C. H. Chang, H. F. Fu, G. L. Wang and J. M. Zhang, Sci. China Phys. Mech. Astron. **58**, 071001 (2015) [arXiv:1411.3428 [hep-ph]].
- [19] T. Zhou, T. h. Wang, Y. Jiang, L. Huo and G. L. Wang, J. Phys. G **48**, 055006 (2021) [arXiv:2006.05704 [hep-ph]].
- [20] D. Ebert, R. N. Faustov and V. O. Galkin, Phys. Rev. D **68**, 094020 (2003) [arXiv:hep-ph/0306306].
- [21] D. Ebert, R. N. Faustov and V. O. Galkin, Phys. Rev. D **82**, 034019 (2010) [arXiv:1007.1369 [hep-ph]].
- [22] M. A. Ivanov, J. G. Korner and P. Santorelli, Phys. Rev. D **73**, 054024 (2006) [arXiv:hep-ph/0602050].
- [23] Y. M. Wang and C. D. Lu, Phys. Rev. D **77**, 054003 (2008) [arXiv:0707.4439 [hep-ph]].
- [24] T. Huang and F. Zuo, Eur. Phys. J. C **51**, 833 (2007) [arXiv:hep-ph/0702147].
- [25] A. Y. Anisimov, I. M. Narodetsky, C. Semay and B. Silvestre-Brac, Phys. Lett. B **452**, 129 (1999) [arXiv:hep-ph/9812514].
- [26] A. Y. Anisimov, P. Y. Kulikov, I. M. Narodetsky and K. A. Ter-Martirosian, Phys. Atom. Nucl. **62**, 1739 (1999) [arXiv:hep-ph/9809249].
- [27] E. Hernandez, J. Nieves and J. M. Verde-Velasco, Phys. Rev. D **74**, 074008 (2006) [arXiv:hep-ph/0607150].
- [28] P. Colangelo and F. De Fazio, Phys. Rev. D **61**, 034012 (2000) [arXiv:hep-ph/9909423].
- [29] I. Bediaga and J. H. Munoz, [arXiv:1102.2190 [hep-ph]].
- [30] Z. Rui, H. Li, G. x. Wang and Y. Xiao, Eur. Phys. J. C **76**, 564 (2016) [arXiv:1602.08918

- [hep-ph]].
- [31] W. F. Wang, Y. Y. Fan and Z. J. Xiao, *Chin. Phys. C* **37**, 093102 (2013) [arXiv:1212.5903 [hep-ph]].
- [32] J. F. Sun, D. S. Du and Y. L. Yang, *Eur. Phys. J. C* **60**, 107 (2009) [arXiv:0808.3619 [hep-ph]].
- [33] M. A. Ivanov, J. G. Korner and P. Santorelli, *Phys. Rev. D* **63**, 074010 (2001) [arXiv:hep-ph/0007169].
- [34] V. V. Kiselev, A. E. Kovalsky and A. K. Likhoded, *Nucl. Phys. B* **585**, 353 (2000) [arXiv:hep-ph/0002127].
- [35] A. Issadykov, M. A. Ivanov and G. Nurbakova, *EPJ Web Conf.* **158**, 03002 (2017) [arXiv:1907.13210 [hep-ph]].
- [36] L. Nayak, P. C. Dash, S. Kar and N. Barik, *Eur. Phys. J. C* **82**, 750 (2022) [arXiv:2204.04453 [hep-ph]].
- [37] Z. Q. Zhang, Z. L. Guan, Y. C. Zhao, Z. Y. Zhang, Z. J. Sun, N. Wang and X. D. Ren, *Chin. Phys. C* **47**, 013103 (2023) [arXiv:2208.07990 [hep-ph]].
- [38] Y. Sakaki, M. Tanaka, A. Tayduganov and R. Watanabe, *Phys. Rev. D* **88**, 094012 (2013) [arXiv:1309.0301 [hep-ph]].
- [39] R. L. Workman *et al.* [Particle Data Group], *Review of Particle Physics*, *PTEP* **2022**, 083C01 (2022).
- [40] A. Berns and H. Lamm, *JHEP* **12**, 114 (2018) [arXiv:1808.07360 [hep-ph]].
- [41] H. Lamm [arXiv:1809.08227 [hep-ph]].
- [42] A. Cerri, *et al.*, *CERN Yellow Rep. Monogr.* **7**, 867 (2019) [arXiv:1812.07638 [hep-ph]].
- [43] M. Tanaka and R. Watanabe, *Phys. Rev. D* **87**, 034028 (2013) [arXiv:1212.1878 [hep-ph]].
- [44] J. P. Lees *et al.* [BaBar Collaboration], *Phys. Rev. D* **88**, 072012 (2013) [arXiv:1303.0571 [hep-ex]].
- [45] M. A. Ivanov, J. G. Korner and C. T. Tran, *Phys. Rev. D* **92**, 114022 (2015) [arXiv:1508.02678 [hep-ph]].
- [46] M. A. Ivanov, J. G. Korner and C. T. Tran, *Phys. Rev. D* **95**, 036021 (2017) [arXiv:1701.02937 [hep-ph]].
- [47] M. Tanaka and R. Watanabe, *Phys. Rev. D* **82**, 034027 (2010) [arXiv:1005.4306 [hep-ph]].
- [48] Y. K. Hsiao and C. Q. Geng, *Chin. Phys. C* **41**, 013101 (2017) [arXiv:1607.02718 [hep-ph]].
- [49] V. V. Kiselev [arXiv:hep-ph/0211021].
- [50] C. H. Chang and Y. Q. Chen, *Phys. Rev. D* **49**, 3399 (1994).
- [51] R. N. Faustov, V. O. Galkin and X. W. Kang, *Phys. Rev. D* **106**, 013004 (2022) [arXiv:2206.10277 [hep-ph]].
- [52] W. Wang, Y. L. Shen and C. D. Lu, *Phys. Rev. D* **79**, 054012 (2009) [arXiv:0811.3748 [hep-

ph]].

- [53] L. Nayak, S. Patnaik, P. C. Dash, S. Kar and N. Barik, *Phys. Rev. D* **104**, 036012 (2021) [arXiv:2106.09463 [hep-ph]].
- [54] Z. R. Huang, Y. Li, C. D. Lu, M. A. Paracha and C. Wang, *Phys. Rev. D* **98**, 095018 (2018) [arXiv:1808.03565 [hep-ph]].